Research Article

A Design and Analysis of a Square Diaphragm-Comb Structure Capacitive Pressure Sensor (SD-CSCPS)

Maibam Sanju Meetei[1,*], Borat Basumatari[2] and Remika Ngangbam[3]

[1]*Department of Electronics and Communication Engineering, Rajiv Gandhi University, India*
[2]*Department of Instrumentation Engineering, Central Institute of Technology Kokrajhar, India*
[3]*Department of Electronics and Communication Engineering, Techno India University, India*

_____

Abstract

This study illustrates the simulation and mathematical analysis of a square diaphragm-comb structure capacitive pressure sensor (SD-CSCPS). The detection of pressure ranges between 10 MPa and 100 MPa with linear output to the applied pressure is the primary emphasis of this research work. In this study, four square diaphragms of same length and breadth with different thickness of 25 μm, 30 μm, 35 μm and 45μm are studied. The construction and design method of a SD-CSCPS using a diaphragm are laid out step-by-step in the design chart. In this study, the square diaphragm is deflected due to applied pressure. This deflection is converted into linear displacement by a mechanical coupler so that the sensor output characteristic can be linearized. The analytical model has two components: the deflection model and the charge model. The deflection of the square diaphragm is computed in deflection model, as this deflection is used to move the movable comb structure. It is highly challenging to determine the absolute capacitance for such a complex construction; instead, the shift in capacitance is calculated in the charge model. The proposed 3D model of the SD-CSCPS was developed and simulated using COMSOL Multiphysics, which also validates the analytical model of SD-CSCPS. Among the various parameters that can increase SD-CSCPS sensitivity are the physical dimensions of the diaphragm, the number of interdigitated fingers of the comb, the dimension of the interdigital finger, the gap between the movable and stationary plates, Poison's ratio, and Young's modulus. In this study, the maximum sensitivity of the sensor with a diaphragm of 25 μm was determined. The simulated and calculated sensitivity of the SD-CSCPS for a diaphragm thickness of 25 μm are 0.253 fF/MPa and 0.319 fF/MPa, respectively.

Keywords: capacitance, deflection, inter-digited, linearity, mechanical coupler, sensitivity.

_____

1. Introduction

A capacitor is a device that stores charge and has two conductor plates, one of which is positively charged and the other negatively charged. The applied electrical potential caused the development of the electric charges present in the conductor plates. The ratio of these electric charges that have been stored to the applied electric potential between the conductor plates is known as capacitance. This capacitance can be varied due to changes in surface area, dielectric material, and the gap between the plates. This fundamental idea serves as the basis for designing the sensor, with one of the parameters serving as a stimulus-dependent variable.

For a basic parallel plate capacitor, the capacitance is inversely proportional to the distance (d) between parallel plates, the directly proportional to the dielectric coefficient (ε), and the length (l) and breadth (b) of the parallel plates. It can be expressed mathematically, as follows

$$C = \varepsilon \frac{lb}{d} \tag{1}$$

There are two types of capacitances: mutual and self-capacitance. Here, the difference in the electric potential generated by the static charge on a body and the ground is used to quantify self-capacitance, or the ability of a body to hold onto charge. The stored charge between two conductors creates mutual capacitance, which is developed by the difference in electric potential between the two conductors. Based on their sensing mechanisms, numerous pressure sensor types are studied in various research works. They are resistive [1-2], capacitive [3-4], inductive [5-7], thermal [8], piezoelectric [9-13], and optical-based [10] pressure sensors. The capacitive pressure sensor is highly compatible with MEMS applications. The three primary types of pressure sensors are based on capacitors. They are capacitive comb structure sensor, touch planer capacitive sensor, and non-touch planar capacitive pressure sensor [2][11-12]. The comparisons between the capacitive comb structure sensor, non-touch planar capacitive pressure sensor, and touch planer capacitive sensor are that the capacitive comb structure sensor has high sensitivity with highly linear, the non-touch planar capacitive pressure sensor has low sensitivity with nonlinear, and the touch planer capacitive sensor has high sensitivity with nonlinear. The comb structure has two types. There is a single-side comb structure and a double-side comb structure. Fig. 1 depicts the double-sided comb-like design of the capacitive pressure sensor, which contains inter-digitated fingers that mimic two interlocking combs. The surface area of the device was enhanced by this construction, which increased the capacitance of the sensor.

In a simple double-sided comb structure design, as shown in Fig. 1, there are a combination ten parallel plate capacitors. These ten capacitors are in parallel connection, after neglecting

_____

the fringing electric field, the total capacitance is given by Eq. 4.

$$C_1 = C_3 = C_5 = C_6 = C_8 = C_{10} \qquad (2)$$

Where, C_1, C_3, C_5, C_6, C_8 and C_{10} are the capacitance form in vertical direction.

$$C_2 = C_4 = C_7 = C_9 \qquad (3)$$

Where, C_2, C_4, C_7 and C_9 are the capacitance form in horizontal direction.

$$C = 4C_2 + 6C_1 \qquad (4)$$

Where, C is the total capacitance in a single unit of comb structure.
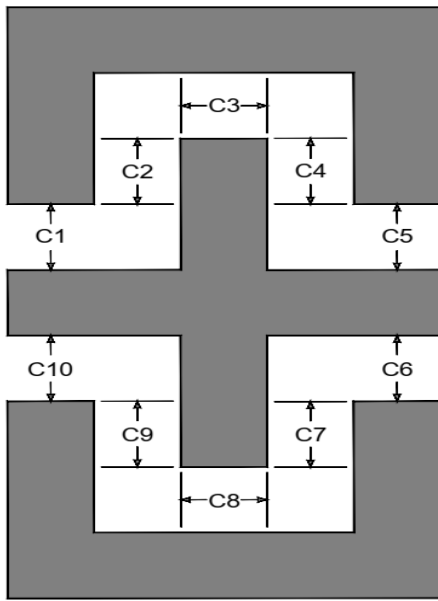
Fig. 1. Capacitors in comb like structure.

The main objective of this study is to designed the capacitive pressure sensor for sensing pressure range from 10 MPa to 100 MPa with highly linear. The Practical Application of the Design can be used in Locomotive Fuel Injection System as the fuel injection has pressure 60-80 MPa bar [14], Aerospace/Rocket Engine and Fuel Monitoring System as high-pressure helium bottles up to 30 MPa are used as prepollent [15], Hydraulic System used analog based pressure gauges in the range of MPa., and Medical System as pressure gauges used in oxygen cylinders & autoclaves are in the rage of MPa. So, it is very important to designed a MEMS based pressure sensor ranges from 10 MPa to 100 MPa.

2. Design Flow

This study suggested a methodology that involves mathematical calculation of the square diaphragm deflection in order to determine the sensor output capacitance for the applied pressure range of 10 to 100 MPa. Next, simulate the proposed model of the sensor using COMSOL Multiphysics for the same applied pressures.

Fig. 2. Design flows of the SD-CSCPS.

The simulated output deflection and analytical deflection values for square diaphragms are then compared and validated. The various parameters that influence the sensitivity of the sensor are found in this research work. The proposed design flow for SD-CDCPS with highly sensitive and linear features is shown in Fig. 2.

3. Analytical Model

In an analytical model, the square diaphragm's deflection is first estimated for the applied pressure in order to identify the various factors that affect the deflection. This deflection is used to move the movable comb with the help of a mechanical coupler. The movement of this movable comb changes the capacitance of the sensor. Then, the overall sensitivity is determined by computing the change in capacitance resulting from the movement of the movable comb structure caused by the deflection.

3.1. Deflection Model
The primary function of the diaphragm is to convert the input pressure into deflection; therefore, the deflection is calculated first. For calculating the deflection of a square diaphragm, let us first consider a rectangular diaphragm, where *2b* represents the length and *2a* represents the width. The distance from its centre along the diaphragm's breadth and length is considered as *a* and *b* along the *x* and *y* axes, respectively. The entire energy (*H*) of the diaphragm under pressure is provided by [16-18].

$$H = \frac{1}{2}\int_{-b}^{b} D \int_{-a}^{a} \left\{ \left(\frac{\partial^2 w}{\partial x^2} + \frac{\partial^2 w}{\partial y^2}\right)^2 - 2(1-v)\left\{\frac{\partial^2 w}{\partial x^2}\frac{\partial^2 w}{\partial y^2} - \left(\frac{\partial^2 w}{\partial x \partial y}\right)^2\right\}\right\} dxdy - \int_{-b}^{b} 1 \int_{-a}^{a} w\, P dxdy. \qquad (5)$$

Where, w is the deflection function, v is the Poisson's

ratio, D is the flexure rigidity, and P is the applied pressure. The value D is given by:

$$D = \frac{Eh^3}{12(1-v^2)}, \tag{6}$$

Where, h is the thickness and E is the Young's modulus.

The deflection of the rectangular diaphragm w is given by:

$$w(x,y) = k(a^2 - x^2)^2(b^2 - y^2)^2 \tag{7}$$

Substituting the value of D and w(x,y) into Eq. 5 and applying the condition $\frac{\partial H}{\partial k} = 0$, the value of k is given by:

$$k = \frac{49P}{128(7a^4 + 4a^2b^2 + 7b^4)D} \tag{8}$$

Substituting the Eq. 8 in Eq. 6, the value of w is given by:

$$w = \frac{49P}{128D(7a^4 + 4a^2b^2 + 7b^4)}(a^2 - x^2)^2(b^2 - y^2)^2 \tag{9}$$

Substituting the value of b by the value of a in Eq. 9 as the length and breadth of square diaphragm are same. The Eq. 9 can be written as:

$$w = \frac{49P}{128D(18a^4)}(a^2 - x^2)^2(a^2 - y^2)^2 \tag{10}$$

Now the above Eq.10 can be written as

$$w = 0.02126\frac{Pa^4}{D}(1 - \frac{x^2}{a^2})^2(1 - \frac{y^2}{a^2})^2 \tag{11}$$

Eq. 11 provides the deflection of a square diaphragm at a given by the value of x and y. For a square diaphragm, the center has the highest deflection value. Now the expression of the maximum deflection $w(x,y)_{max}$ is given by:

$$w(0,0) = w(x,y)_{max} = 0.02126\frac{Pa^4}{D} \tag{12}$$

Substituting Eq. 5 in Eq. 12, Eq. 12 can be rewritten as:

$$w(x,y)_{max} = 0.25512\frac{Pa^4(1-v^2)}{Eh^3} \tag{13}$$

From Eq. 11, it is found that the diaphragm deflection depends on the input pressure, dimensions of the square diaphragm, Poisson's ratio, and Young's modulus.

3.2. Charge Model

The lateral view of the SD-CSCPS is shown in Fig. 3, and the top view of the comb structures is illustrated in Fig. 4. This structure consists of a square diaphragm, a movable comb, a stationary comb, and a mechanical coupler. The diaphragm function is to transform the input pressure into deflection as a result of the pressure that is being applied to it. The mechanical coupler moves the movable comb linearly by transforming the deflection into linear movement.

It also acts as an isolator between the diaphragm and the movable comb. The linear displacement between the moving and stationary comb plates is converted into a change in the capacitance of the capacitive comb.
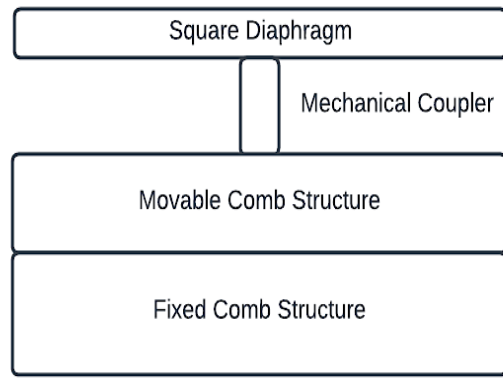
Fig. 3. Lateral views of SD-CSCPS.
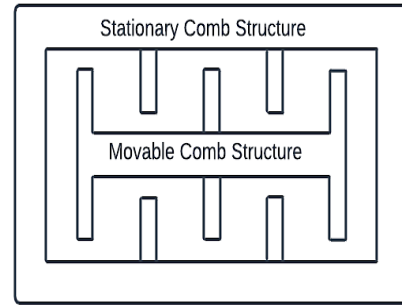
Fig. 4. Top view of the Comb structure.

From Fig. 1, the capacitance change (ΔC) for the comb structure can be express as below:

$$\Delta C = 4\Delta C_2 + 6\Delta C_1 \tag{14}$$

The value of and are given by:

$$\Delta C_1 = \varepsilon_0 \frac{b_1 w}{d} \tag{15}$$

$$\Delta C_2 = \varepsilon_0 \frac{l_2 w}{d} \tag{16}$$

Where, ε_o is the absolute permittivity, b_1 is the breath of C_1, l_2 is the length of C_2, and d is the gap between the movable and stationary comb structure. If the inter-digital comb fingers of the comb structure are increased by n, then the value of the sensor is:

$$\Delta C_n = 4n\left(\varepsilon_0 \frac{l_2 w}{d} + \varepsilon_0 \frac{b_1 w}{d}\right) + 2\varepsilon_0 \frac{b_1 w}{d} \tag{17}$$

The sensor's sensitivity (S) can be calculated by

$$S = \frac{4n\left(\varepsilon_0 \frac{l_2 w}{d} + \varepsilon_0 \frac{b_1 w}{d}\right) + 2\varepsilon_0 \frac{b_1 w}{d}}{P} \tag{18}$$

The sensor's sensitivity is a function of the n numbers of inter-digital fingers, the l_2 length and b_1 breadth of the capacitance, the w deflection that causes a change in the position of the movable comb structure, the d gap between the plates, and the ε_o absolute permittivity.

4. Simulation of SD-CSCPS 3D model

The COMSOL Multiphysics software is used in this study to simulate the proposed SD-CSCPS design model. In this simulation, the physics used is electromechanics physics and choose the study as stationary. In global definitions, the input

pressure is declared in the parameter section. In the geometry section, the model of the proposed sensor is described.

In the material section, the various materials for each component of the model are assigned, such as gold (Au) for the movable, fixed comb structure, silicon (Si) for square diaphragm and silicon dioxide (SiO_2) for the mechanical coupler. The reason for using silicon as diaphragm material are excellent mechanical properties as it has high elastic modulus of 180 GPa that make it robust and rigid, compatible with MEMS fabrication and thermal stability. The reasons for selecting silicon dioxide as a mechanical coupler material are that it is an excellent dielectric material and can be used as an insulating material; it is also compatible with silicon fabrication; and it also has high thermal and chemical stability. The reasons for selecting gold as a comb structure material are that it has a good conductor with low contact resistance, high corrosion resistance, and good surface bonding with other materials.

The simulation is carried out for the sensor with a diaphragm length of 300 μm and different diaphragm thicknesses ranging from 25 μm to 40 μm with a step size of 5 μm.

After assigning the materials, the physics configurations like fixed constraint, boundary load, ground, and terminal are configured accordingly. After the configuration of the physics, the meshing of the designed sensor is done in a tetrahedral shape. The size of the meshing of the designed sensor is taken as fine. The applied pressure to the sensor for the study ranges from 10 MPa to 100 MPa with a step size of 10 MPa and is declared in the parameter swap under the study section.
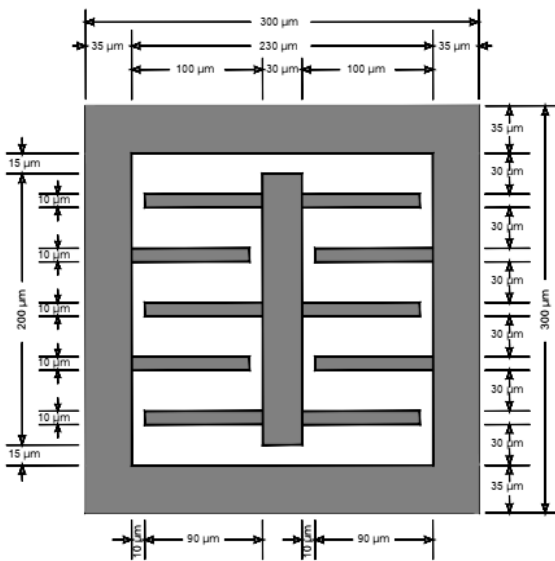
Fig. 5. Dimension of the movable and non-movable comb structures.

The dimension of the movable and non-movable comb structures used in the simulation is shown in Fig. 5.

5. Result and Discussion

An input pressure of 10 MPa to 100 MPa with a gap of 10 MPa is used for the analysis of the sensor. In this study, the diaphragm thickness of 25 μm to 40 μm is considered. The various reasons for selecting these thickness ranges are: If the diaphragm thickness is higher, then the sensor will be less sensitive to the pressure variation, but they can handle more pressure without mechanical failure. If the sensor has a lesser

thickness, the sensor will have higher sensitivity, but they cannot handle more pressure because of mechanical failure. In MEMS technology, the diaphragm of the silicon is generally 25 μm to 75 μm by ensuring to withstand enough stress and strain induced on the diaphragm.

Fig. 6 displays the simulated output deflection for the square diaphragm with a thickness of 25 μm for applied pressure at 100 MPa. This Fig. 4 shows the maximum deflection occurred at the center of the diaphragm with a value of 8.30 μm, which is consistent with the findings of the mathematical model. The deflection of the diaphragm is translated into linear displacement by the mechanical coupler.
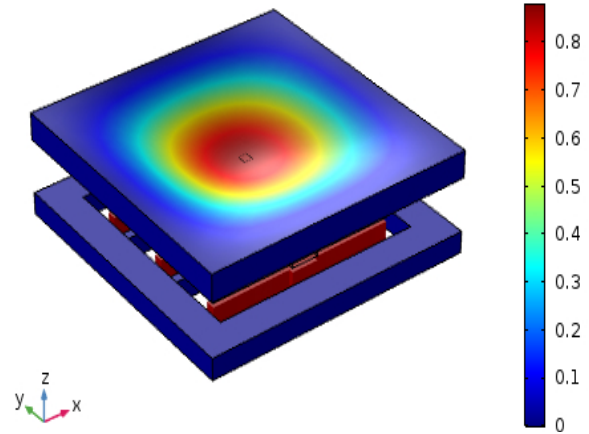
Fig. 6. Simulated output showing the deflection of the diaphragm at 100 MPa.

Table 1. Deflection values in μm.

Thick	25 μm		30 μm		35 μm		40 μm	
Pres* (MPa)	Sim*	Cal*	Sim	Cal	Sim	Cal	Sim	Cal
10	0.87	0.83	0.53	0.48	0.36	0.30	0.25	0.20
20	1.75	1.66	1.06	0.96	0.72	0.60	0.51	0.40
30	2.61	2.49	1.60	1.44	1.07	0.90	0.76	0.60
40	3.47	3.32	2.13	1.92	1.43	1.21	1.02	0.81
50	4.31	4.16	2.66	2.40	1.79	1.51	1.28	1.01
60	5.15	4.99	3.19	2.88	2.14	1.81	1.53	1.21
70	5.96	5.82	3.72	3.37	2.50	2.12	1.79	1.42
80	6.76	6.65	4.25	3.85	2.85	2.42	2.05	1.62
90	7.53	7.48	4.76	4.33	3.20	2.72	2.30	1.82
100	8.30	8.32	5.27	4.81	3.56	3.03	2.56	2.03

Pres*: Pressure   Sim*: Simulated value   Cal*:Calculated value
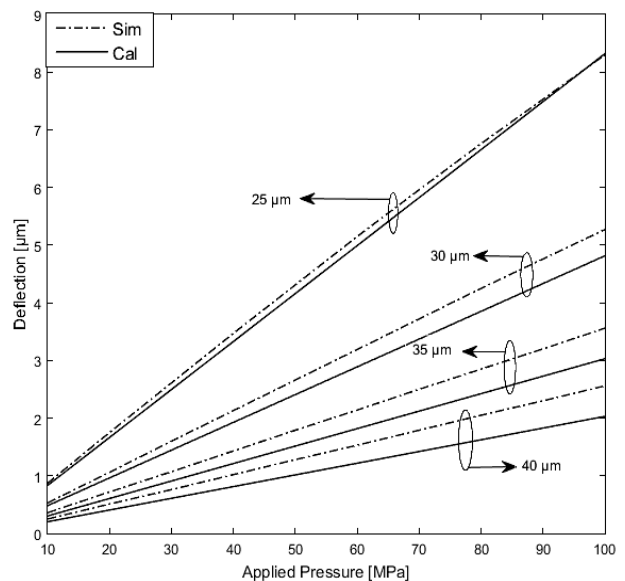
Fig. 7. Simulated and Calculated Displacements for SD-CSCPS with Different Diaphragm.

Table 1 shows the simulated and analytical output deflection of the CD-CSCPS for different diaphragm thickness for the applied pressure range from 10 MPa to 100 MPa. This table also makes it obvious that the deflection increases as applied pressure increases. The simulated deflection values and the calculated deflection values are similar at the same applied pressure level.

The graphic representations of Tab. 1 are shown in Fig. 7. In this figure, it is observed that the output deflection is linearly proportional to the applied pressure. It is also detected that the output characteristic is highly linear to the applied pressure. For sensors with a smaller thickness, the slope is steeper means higher the deflection. This means sensitivity is higher for lower thickness.

It is also observed that the simulated output values of deflection and the calculated values of deflection are very close to each other. So, this mean that the deflection equation and simulation are validated as minor deviations in between them.

Table 2. Capacitance values in fF.

Thi-ck	25 µm		30 µm		35 µm		40 µm	
Pre-ssure (MPa)	Sim	Cal	Sim	Cal	Sim	Cal	Sim	Cal
10	0.29	0.31	0.20	0.18	0.17	0.11	0.13	0.07
20	0.56	0.63	0.36	0.37	0.28	0.23	0.21	0.15
30	0.82	0.95	0.53	0.55	0.38	0.34	0.29	0.23
40	1.08	1.27	0.69	0.74	0.49	0.46	0.37	0.31
50	1.34	1.59	0.85	0.92	0.60	0.58	0.44	0.39
60	1.59	1.91	1.01	1.11	0.71	0.69	0.52	0.46
70	1.84	2.23	1.17	1.29	0.82	0.81	0.60	0.54
80	2.07	2.55	1.33	1.48	0.92	0.93	0.68	0.62
90	2.30	2.87	1.49	1.66	1.03	1.04	0.76	0.70
100	2.52	3.19	1.64	1.85	1.14	1.16	0.83	0.78

In Table 2, the designed CD-CSCPS's simulated and calculated output capacitances for various diaphragm thicknesses are shown. This table demonstrates how closely the simulated and calculated values of capacitance change are related. As a result, the suggested equation for capacitance variations in CD-CSCPS is verified and useful for designing such sensors. It is also observed that the higher the change in output capacitance, the lower the diaphragm thickness.

Table 2 can be illustrated in graphical form, as shown in Fig. 8. This graph demonstrates that the sensor's change in capacitance is very linear, which is a desired result. This graphic also shows that the sensor's sensitivity increases as the diaphragm's thickness is reduced. It also demonstrates that the sensitivity of the 25 µm thick CD-CSCPS is 0.253 fF/MPa and 0.319 fF/MPa, respectively, for simulation and calculation.
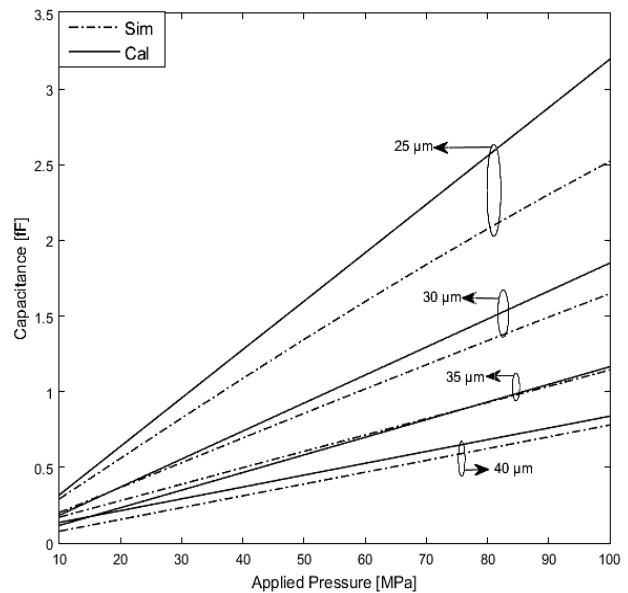
Fig. 8. Simulated and Calculated Capacitance for SD-CSCPS with Different Diaphragm.

6. Conclusion

The analytical modelling and simulation of the CD-CSCPS for detecting input pressure ranging from 10 MPa to 100 MPa is the primary objective of this research work. It is suggested and implemented as a design method for a CD-CSCPS. The suggested design approach can be used in subsequent designs because the analytical and simulated deflection and change in capacitance values are so close.

When the thickness of the diaphragm decreases, the sensitivity increases. The length increases the diaphragm deflection, resulting in increased sensitivity for the sensor. The sensor's sensitivity is also influenced by Young's modulus and Poisson's ratio. There is an increase in the output capacitance with an increase in the comb fingers' dimension and number. As the gap between the movable comb and the stationary comb gets smaller, the sensitivity also increases. The proposed sensor model has a linear output characteristic. The sensitivity of the proposed CD-CSCPS for a diaphragm thickness of 25 µm is 0.253 fF/MPa and 0.319 fF/MPa, respectively.

References

[1] S.-P. Chang, J.-B. Lee, and M. G. Allen, "Robust capacitive pressure sensor array," *Sens. Actuat. A: Phys.*, vol. 101, no. 1–2, pp. 231–238, Sep. 2002, doi: 10.1016/S0924-4247(02)00193-0.

[2] L. Shu, X. Tao and D. D. Feng, "A New Approach for Readout of Resistive Sensor Arrays for Wearable Electronic Applications," *in IEEE Sensors Journal,* vol. 15, no. 1, pp. 442-452, Jan. 2015, doi: 10.1109/JSEN.2014.2333518.

[3] D. P. J. Cotton, I. M. Graz and S. P. Lacour, "A Multifunctional Capacitive Sensor for Stretchable Electronic Skins," *IEEE Sens. J.*, vol. 9, no. 12, pp. 2008-2009, Dec. 2009, doi: 10.1109/JSEN.2009.2030709.

[4] M. S. Meetei, N. Naga, N. Taji and R. Sharma, "Modelling and Simulation of Square Diaphragm Touch Mode Capacitive Pressure

Sensor," *Int. J. Mech. Eng.*, vol. 8, no. 1, pp. 13-21, Jan. 2023

[5] E. G. Bakhoum and M. H. M. Cheng, "High-Sensitivity Inductive Pressure Sensor," *IEEE Trans. Instrum. Meas.*, vol. 60, no. 8, pp. 2960–2966, Aug. 2011, doi: 10.1109/TIM.2011.2118910.

[6] S. C. Bera, N. Mandal and R. Sarkar, "Study of a Pressure Transmitter Using an Improved Inductance Bridge Network and Bourdon Tube as Transducer," *IEEE Trans. Instrum. Meas*, vol. 60, no. 4, pp. 1453-1460, April 2011, doi: 10.1109/TIM.2010.2090697.

[7] L. Pan, A. Chortos, G. Yu, Y. Wang, S. Isaacson, R. Allen, Y. Shi, R. Dauskardt and Z. Bao, "An ultra-sensitive resistive pressure sensor based on hollow-sphere microstructure induced elasticity in conducting polymer film," *Nat. Commun.*, vol. 5, no. 3002, Jan. 2014, doi: 10.1038/ncomms4002.

[8] X. Wang et al., "A Flexible Thin-Film Pressure Sensor Based on Thermal Conduction Mechanism for Pressure, Orientation, and Mapping Signal Acquisition," *IEEE Sensors J.*, vol. 23, no. 3, pp. 1990-1998, 1 Feb.1, 2023, doi: 10.1109/JSEN.2022.3230982.

[9] M. S. Meetei, A. D. Singh and S. Majumder, "A Novel Design Approach for Beam Bridge Structure Pressure Sensor Base on PZT-5A Piezoelectric," *J. Enh. Sci. Techn. Rev.*, vol. 14, no. 1, pp. 193–199, Jan. 2021, doi:10.25103/jestr.141.23.

[10] J. W. Arkwright, I. D. Underhill, S. A. Maunder, A. Jafari, N. Cartwright and C. Lemckert, "Fiber Optic Pressure Sensing Arrays for Monitoring Horizontal and Vertical Pressures Generated by Traveling Water Waves," *IEEE Sensors J.*, vol. 14, no. 8, pp. 2739-2742, Aug. 2014, doi: 10.1109/JSEN.2014.2311806.

[11] S. Guo, J. Guo and W. H. Ko, "A monolithically integrated surface micromachined touch mode capacitive pressure sensor," *Sens. Actuat. A: Physic.*, vol. 80, no. 3, pp. 224–232, Mar. 2000, doi: 10.1016/S0924-4247(99)00344-1.

[12] V. Tsouti, G. Bikakis, S. Chatzandroulis, D. Goustouridis, P. Normand and D. Tsoukalas, "Impact of structural parameters on the performance of silicon micromachined capacitive pressure sensor,"

Sens. Actuat. A: Physic., vol. 137, no. 1, pp. 20–24. June 2007, doi: 10.1016/j.sna.2007.02.015.

[13] S. M. Singh, K. P. Kalita and S. M. Meetei, "Piezoelectric-Based Square Diaphragm Pressure Sensor Modelling and Analysis using PZT-5H and PZT-5A," *SSRG Int. J. Elec. Elec. Eng,* vol. 10, no. 8, pp. 1-8, Aug. 2023, doi: 10.14445/23488379/IJEEE-V10I8P101.

[14] R. D. Reitz and G. Duraisamy, "Review of high efficiency and clean reactivity controlled compression ignition (RCCI) combustion in internal combustion engines", *Progr. Ener. Combus. Sci.*, vol. 46, pp.12-71, Feb. 2015, doi: 10.1016/j.pecs.2014.05.003.

[15] O. Haidn, "Advanced Rocket Engines", Advances in Propulsion Technology for High-Speed Aircraft," *in Adv. Propul. Techn. High-Speed Aircr.,* vol. 6, pp. 1-60, Sep. 2007.

[16] A. C. Ugural, "*Plates and Shells: Theory and Analysis,*" Boca Raton, London, New York: CRC Press, 2017.

[17] M. Bao, "*Analysis and Design Principles of MEMS Devices*", 1st ed. Sanghai, China: Elsevier Science, 2005.

[18] S. Timoshenko, P. Stephen and K. Woinowsky, "*Theory of Plates and Shells*" 2nd ed., New York, USA: McGraw Hill, 1989.